High performance InP Geiger-mode SWIR avalanche photodiodes

Ping Yuan[1], Rengarajan Sudharsanan, Joseph Boisvert, Xiaogang Bai, Paul McDonald, Takahiro Isshiki, William Hong
Boeing Spectrolab Inc. 12500 Gladstone Ave. Sylmar, CA 91342

Michael Salisbury
Boeing SVS Inc., 4411 The 25 Way NE # 350 Albuquerque, NM 87109

Chong Hu, Mingguo Liu, and Joe C. Campbell
University of Virginia, Electrical and Computer Engineering, 351 McCormick Rd
Charlottesville, VA 22904-4743

ABSTRACT

LAser Detection And Ranging (LADAR) is a promising tool for precise 3D-imaging, which enables field surveillance and target identification under low-light-level conditions in many military applications. For the time resolution and sensitivity requirements of LADAR applications, InGaAsP/InP Geiger-mode (GM) avalanche photodiodes (APDs) excel in the spectrum band between 1.0~1.6 μm. Previously MIT Lincoln Laboratory has demonstrated 3D LADAR imaging in the visible and near infrared (1.06 μm) wavelengths with InP/InGaAsP GM-APD arrays. In order to relieve the design tradeoffs among dark count rate (DCR), photo detection efficiency (PDE), afterpulsing, and operating temperature, it is essential to reduce the DCR while maintaining a high PDE. In this paper we will report the progress of GM-APD detectors and arrays with low DCR and high PDE at 1.06 μm.

In order to improve both DCR and PDE, we optimized the multiplication layer thickness, substrate, and epitaxial growth quality. With an optimized InP multiplier thickness, a DCR as low as 100 kHz has been demonstrated at 4V overbias at 300 ^{o}C. and at 240 K, less than 1 kHz DCR is measured. A nearly 40% PDE can be achieved at a DCR of 10 kHz at the reduced temperature.

Keywords: Avalanche photodiode, Geiger Mode, Photon counting, LIDAR, Focal plane array, 3D imaging, photodetector.

1. INTRODUCTION

Due to the recent application developments in three-dimension imaging, quantum cryptography, and time-resolved spectroscopy, single-photon counting avalanche photodiodes (APD) in the short wavelength infrared have attracted a lot interest. Because of the bandgap limit, silicon Geiger-Mode (GM) APDs are not very efficient at 1.06 μm where high power emitters are available. Important figure-of-merits for GM-APDs include dark count rate (DCR) and photon detection efficiency (PDE). The former establishes a noise and false event rate floor for the entire sensor system, and PDE defines the sensor's sensitivity to a single photon. The InP/InGaAsP SAM structure introduced by MIT-LL has demonstrated a good performance balance at this wavelength. In order to improve the GM-APD performance and uniformity for image array applications, we optimized the epitaxial growth, process, and device design for the Geiger-mode operation, and achieved an excellent DCR and PDE balance.

[1] Email: ping.yuan@Boeing.com

Advanced Photon Counting Techniques III, edited by Mark A. Itzler, Joe C. Campbell,
Proc. of SPIE Vol. 7320, 73200P · © 2009 SPIE · CCC code: 0277-786X/09/$18 · doi: 10.1117/12.821284

2. DEVICE STRUCTURE

The device structure follows the traditional separate absorption and charge multiplication (SACM) design: using InGaAsP as the absorber for 1.06 μm and InP as the multiplication layer. A low electric field is applied throughout this low band-gap absorber layer to minimize the tunneling and avalanche multiplication while keep carriers drift in the proper direction. The multiplication layer has to be exposed to a high internal field in order to promote the impact ionization of photo-carriers. A precisely controlled charge layer is inserted between these two layers.

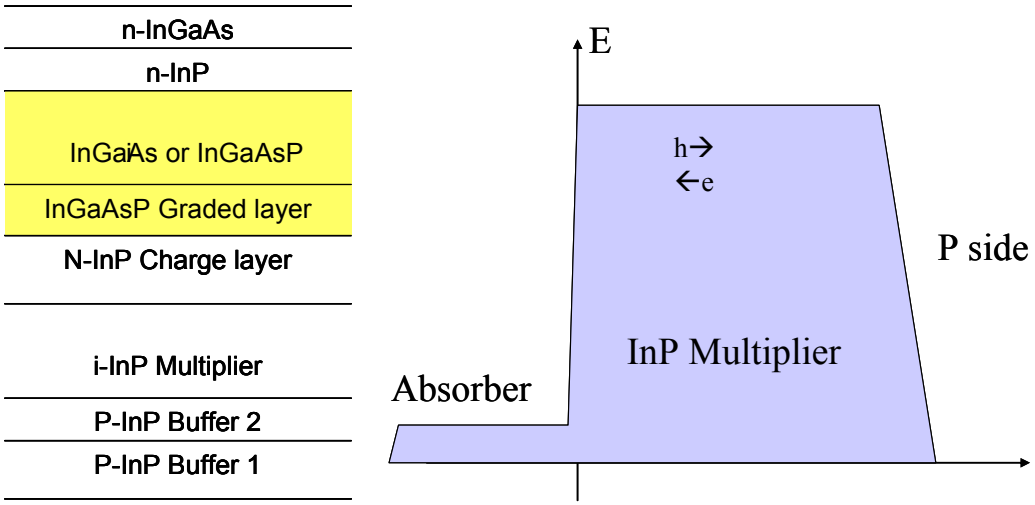

Figure 1 The cross section of the InP/InGaAsP Geiger-Mode APD epitaxial stack and its typical electric field profile at operation. For the following analysis, the origin is at the InP charge and multiplier interface.

The InP/InGaAsP APD structure cross section is shown in Figure 1, and the right figure shows the resultant electric field profile at the operating bias. The thin heavily doped InGaAs capping layer was grown for good ohmic contacts. Under this layer is an N-doped InP window layer, followed by an InGaAsP absorber layer. The material quality and doping level of this narrow band material were closely monitored to minimize the thermal generation and avoid excess electric field and carrier traps. The thickness and doping of the n-type charge layer were carefully controlled. At the bottom is a heavily doped p-type InP layer, followed by an InP buffer layer, also heavily doped.

3. GEIGER-MODE OPERATION

Figure 2 shows a typical current-voltage characteristics of an InP/InGaAsP APD. As the bias voltage reaches the breakdown voltage, the device currents, dark or photo, approach infinity, or the current compliance in practice because of the carrier avalanche ionization. So, it is impossible to bias an APD beyond the breakdown voltage for a long time. However, since it takes some time for the injection to take place and for the avalanche process to build up, it is possible to bias the device for a short period and quench the current once it reaches a certain threshold. The resultant short current pulse will be amplified in the following circuit and registered as an event. If the photon generated injection dominates the carrier injection into the multiplier, the APD can serve as a good single photon detector.

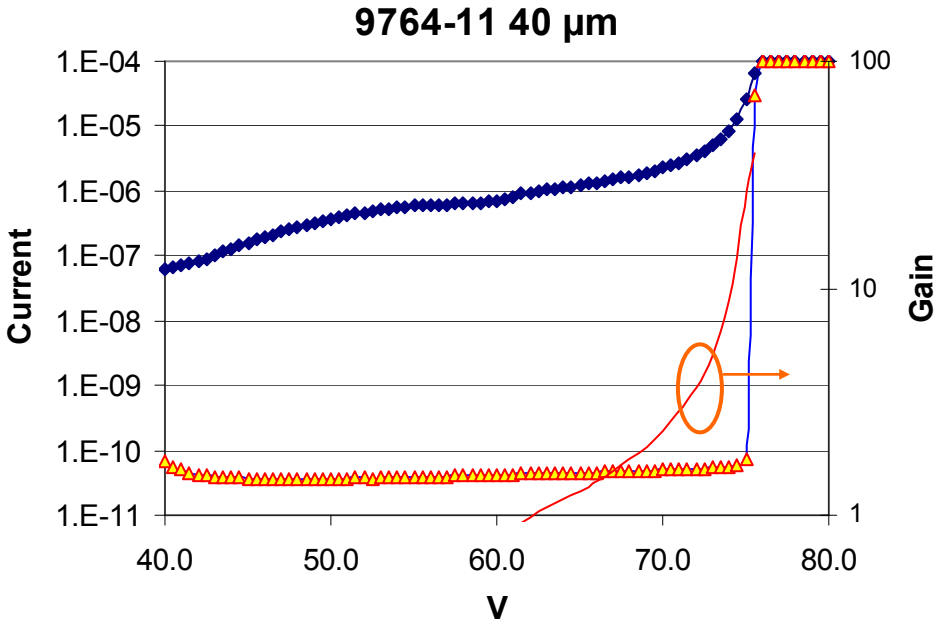

Figure 2 The current-voltage and gain characteristics of a 40 µm Spectrolab InP/InGaAsP 1.06 µm GM APD.

Photon detection efficiency, which is the ratio of the resultant pulses to the incident photons, describes the APD photon sensitivity at the single photon level. Following the photo carrier generation and multiplication process, we can identify the four factors influencing PDE. They are the absorber's absorption efficiency $\eta_{abs}=(1-\exp^{-aWa})$, which is a function of the absorption coefficient a and absorber thickness W_a, the transportation efficiency η_{tran}, the injection efficiency η_{inj}, and avalanche probability P(0) for a hole injection at the absorber and multiplier interface as shown in Figure 1. So,

$$PDE = \eta_{abs}\eta_{tran}\eta_{inj}P(0). \quad (1)$$

In the SAM APD structure, there is a low electric field in the absorber and the InP/InGaAsP interface such that the transportation efficiency η_{tran} and the injection efficiency η_{inj} are close to 1. The absorption efficiency η_{abs} is mainly determined by the absorber thickness, and it is normally controlled to be greater than 70%. So, PDE is primarily determined by P(0) in a SAM structure.

In the following analysis, we will employ the McIntyre APD theory because most of the Geiger-mode APDs are based on a thick multiplier, where the local ionization model is fairly accurate[1]. In the end, we see the advantage of thick multipliers, which explains its popularity in this application. Based on McIntyre's analysis, P(0) is a function of the electron ionization coefficient α, the hole ionization coefficient β, and the multiplier thickness W_m. However, even in a constant electric field, it has to be numerically solved. In practice, P(0) has to be controlled to nearly 50% for an PDE in the range of 30~40%.

In the absence of incident photon, there is still a probability for the GM-APD to break down, or dark count rate (DCR), due to the carrier injections from the thermal generation and tunneling in the absorber region, carrier detrapping at the absorber and multiplier interface, and tunneling in the multiplier. With a careful bandgap and electric field design, the dark generation in the absorber and detrapping at the interface can be well controlled at

reduced temperatures. In practice, the carrier tunneling in the multiplier dominates the dark count generation at the operation condition in a 1.06 μm GM device.

The multipliers of most SAM APD structures are unintentionally doped and the electric field is nearly constant. Based on McIntyre's theory[1], the avalanche probability of an e-h pair injection at x in a constant field E is

$$P(x) = \frac{1}{1 + \frac{1 - P(0)}{P(0)} e^{(\beta - \alpha)x}} = \frac{1}{1 + \frac{1 - P(0)}{P(0)} e^{x / L_{\alpha\beta}}} \tag{2}$$

where $L_{\alpha\beta}=1/(\beta-\alpha)$ and characterizes the decay of P(x) in the multiplier. Because P(0), α and β are functions of E, P(x) is eventually determined by E and x. The band-to-band tunneling generation through a parabolic barrier is described by[2,3]

$$\begin{aligned} G_{mul}(x) &= AE^2 \exp(-\frac{BE_g^{3/2}}{E}) \\ A &= \frac{e^2 \sqrt{\frac{2m_r}{eE_g}}}{4\pi^3 \hbar^2}, B = \frac{\pi \sqrt{m_r / 2}}{2e\hbar}, m_r = \frac{2m_c m_{lh}}{m_c + m_{lh}} \end{aligned} \tag{3}$$

where m_c is the conductance band effective mass and m_{lh} is the light hole effective mass. Then, the DCR due to tunneling in the multiplier with a constant field is

$$\begin{aligned} \int_0^{W_m} dx G_{mul}(x) P(x) &= G_{mul}(x) W_m \left[1 - \frac{L_{\alpha\beta}}{W_m} \ln \frac{1 + K e^{W_m / L_{\alpha\beta}}}{1 + K} \right] = G_{mul}(x) W_m R \\ K &= \frac{1 - P(0)}{P(0)} \approx 1 \end{aligned} \tag{4}$$

Combining the above dark count generation mechanisms, we can get the total DCR of a device with an area of S in a constant field

$$DCR = S\left[G_{mul}(E) W_m R + G_{abs} w_{abs} P(0) + G_{trap} P(0) \right] \tag{5}$$

The ratio of Eq. 5 and 1 gives the DCR equivalent flux (DEF) in the gate period, which is an important figure of merit of photon-counting devices. Based on the equation below,

$$DEF = \frac{DCR}{PDE} = \frac{S}{\eta_{abs}} \left(G_{mul}(E) \frac{W_m R}{P(0)} + G_{abs} w_{abs} + G_{trap} \right) \tag{6}$$

a higher quantum efficiency η_{abs} is always preferable, but the background doping in the actual growth limits the absorber thickness to 1-2 μm for a better electric field control. For an efficient optical coupling, there is also a limit in reducing the device area S. It is important to pursue the best crystal quality to reduce all the generations, G_{mul}, G_{abs}, and G_{trap}, but the product of GWR indicates another avenue to improve the device performance while the multiplier thickness is subject to optimization. As the thickness of the multiplier W_m increases, the electric field decreases, as does the tunneling generate rate G_{mul}. Based on the reported α and β of InP at room temperature[4], the breakdown electric field and breakdown voltage were plotted as a function of the thickness in the left panel of Figure 3. In the same thickness range, the tunneling injection efficiency R shown in Equation 4 and the product of GWR were illuminated in the right panel. As the electric field decreases, the tunneling injection efficiency R

changes little and maintains a value around 0.40 to 0.42 for InP, and the decrease of the tunneling generation dominates the trend over the increase of thickness W_m. A very similar R value and the same trend with the multiplier thickness were obtained with another set of reported α and β of InP[5], though there is considerable difference in the absolute values between the two ionization data sets. So, based on the above analysis, a thicker multiplier with a lower breakdown electric field is preferable to achieve a lower DEF performance at room temperature. Due to the difficulty in obtaining the low-temperature ionization coefficient data[3], the above analysis was not carried to lower temperatures. However, based on observation that the dark count rate of all InP GM APDs decreases with about the same rate over temperature, the room-temperature performance can serve as a good guidance in the device optimization.

4. GROWTH AND PROCESS

The APD structures were grown on two-inch InP substrates in a multi-wafer MOVPE production reactor. Trimethylindium (TMIn), trimethylgallium (TMGa), arsine (AsH3) and phosphine (PH3) were used as sources for In, Ga, As, and P, respectively. Silicon and zinc were used as n- and p- type dopants, respectively. The growth parameters, such as growth temperature, V/III ratio, and dopant concentration, were optimized for the lattice-matched InP and InGaAsP layers with the designed thicknesses and doping concentrations. X-ray diffraction, Dektak, electrochemical-capacitance–voltage (ECV), photoluminescence, and SIMS techniques were employed to characterize the as-grown wafers.

A Bromine/Methanol solution was used to etch the device mesa. Polyimide and SiNx layers were deposited onto the sidewalls to cap and seal the devices. The typical Ti/Pt/Au and Au/Ge/Ni/Au metal stacks were deposited for p and n contacts, respectively. Backside processing was standard for making n type contacts. For the front-side illuminated devices, a more complex process sequence was needed for the front contact. Anti-reflection (AR) layers were typically single quarter wave stacks tuned to the desired wavelength.

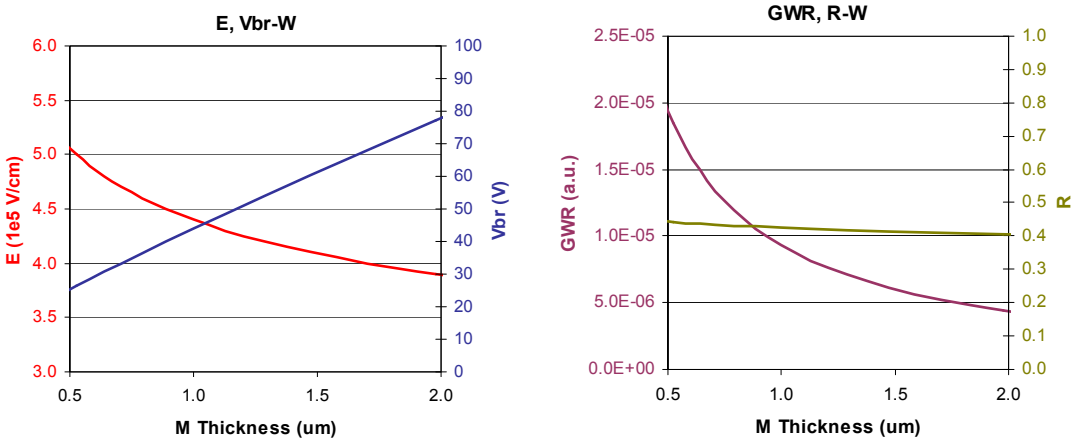

Figure 3 The breakdown electric field and voltage are plotted as a function of the undoped InP multiplier thickness at room temperature. Appreciable decrease in the electric field is observed. Based on the reported ionization coefficients, the tunneling carrier injection efficiency R and the product of GWR are calculated as a function of the multiplier thickness. In the thickness range of interest, the decrease of G_{mul} dominates the trend over the increase of W_m while R keeps nearly constant.

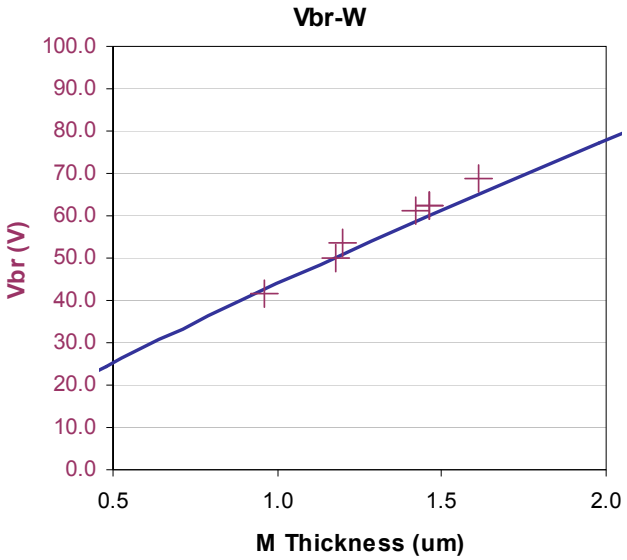

Figure 4 The curve shows the calculated breakdown voltage as function of the undoped InP multiplier thickness at room temperature based on the ionization coefficients reported in Ref. 4. This is the same curve shown in the left panel of Figure 3. The measured Vbr and multiplier thickness of the fabricated devices were illuminated with crosses in the Vbr-M space, and show a good agreement

5. RESULTS AND DISCUSSIONS

In the device structure optimization, a series of InP/InGaAsP GM APD with various multiplier thicknesses were grown and processed. The dark current and photo response of the GM APDs were characterized with a computer-controlled Keithley 238 source meter. For simplicity and accuracy, the 1.06 μm laser beam in a single mode fiber was coupled through a lens and the AR coated surface of the front illuminated devices. Figure 2 illustrated the I-V curves of a 40-μm-diameter device measured at room temperature. The dark current stays below 100 pA before breakdown, which is essential for a low DCR. A punch-though can be observed in the photo response at about 63V, and above this bias the absorber is fully depleted, but it also provides a low field across the absorber even beyond breakdown. An appreciable gain was measured before breakdown, and it implies a good PDE when the device is biased in the Geiger mode. In order to overcome some unintended doping in the absorber and keep a good PDE at low temperature, a reasonable separation before the punchthrough and breakdown has to be maintained. The CV characteristics were measured with an Agilent E4980A and a Keithley 590. The InP multiplier and InGaAsP absorber thicknesses can be determined by the CV results. In order to compare with the thickness-vs-breakdown voltage curve shown in Figure 3, the voltage drop across the absorber has to be subtracted from the total device breakdown voltage. The voltage applied to the multiplier at breakdown can be deduced with the two thicknesses, the punchthrough and breakdown voltages. In Figure 4 experimentally determined breakdown voltage and layer thickness were plotted against the calculated curved based on the ionization data from Ref. 4. A good agreement was achieved, and it also helps to verify the accuracy of the ionization coefficient data used in the above analysis, at least in the electric field range of interest.

In Geiger-mode DCR and PDE measurements operation, the APD is biased to just below the breakdown voltage, and an overbias pulse of a few volts is applied in a gate time of a few nanoseconds. The room-temperature DCR performance of the 1.06 μm APDs fabricated at Spectrolab is shown in Figure 5. For the convenience of comparison, all the devices have a diameter of 30 μm. In a series of effort, the thickness of the multiplier ranges

from about 1.0 µm to 1.6 µm. Coupled with the improvements in growth and substrates, the DCR of the 30 µm APDs improved from nearly 1 MHz at 4V overbias to 100 kHz at room temperature.

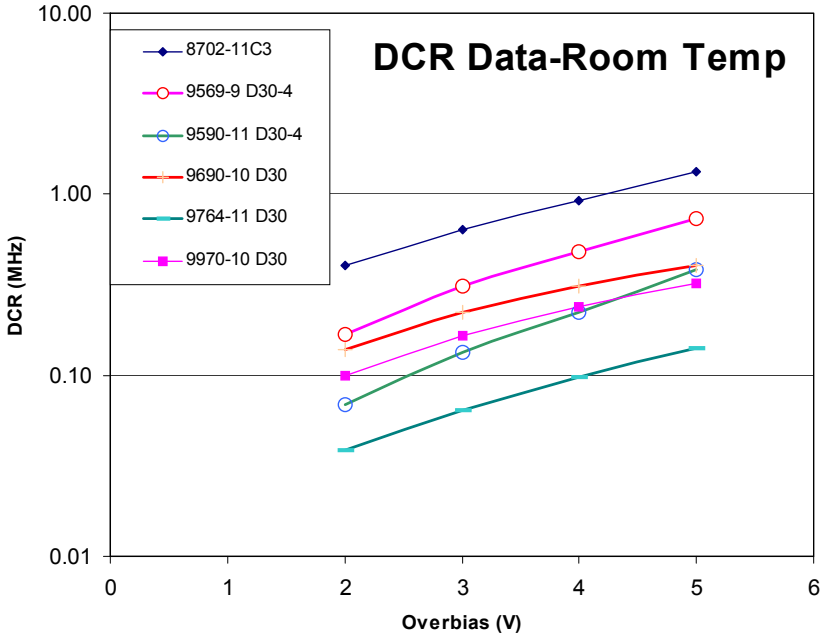

Figure 5 The DCR at room temperature versus overbias characteristics taken on a series of of InGaAsP-InP GM-APDs. The thickness of the multipliers ranges from 1.0 µm to 1.6 µm. With other improvements in growth and substrates, the DCR is reduced by a decade to about 100 kHz at 4 V overbias at room temperature.

The temperature variation of DCR of three typical devices was measured at MIT-LL. As shown in Figure 6, starting from about the same DCR difference at room temperature, the DCR of all the devices decreases with about the same ratio over the temperature. For comparison, all the data shown in Figure 6 were measured at 4V overbias on 30 µm devices. At 240 K, the DCR of Spectrolab 9764 is reduced to less than 1 kHz at 4 V overbias. Compared with our earlier effort with 8702 and 9569, the improvement in DCR is greater than a decade at the reduced temperature.

As is well known[6], both DCR and PDE decrease with overbias and temperature. For the best trade-off of the operation conditions for the GM-APDs, the photon detection efficiency (PDE) were measured as a function of overbias and plotted versus DCR as shown in Figure 7. The PDE data were measured with 1.06 µm laser pulses shorter than 1 nanosecond, and the overbias gate pulses were carefully synchronized with these laser pulses. 9764 series 1.06 µm GM-APDs demonstrated an efficiency nearly 40% with a DCR of about 10 kHz at 250 ^{o}C.

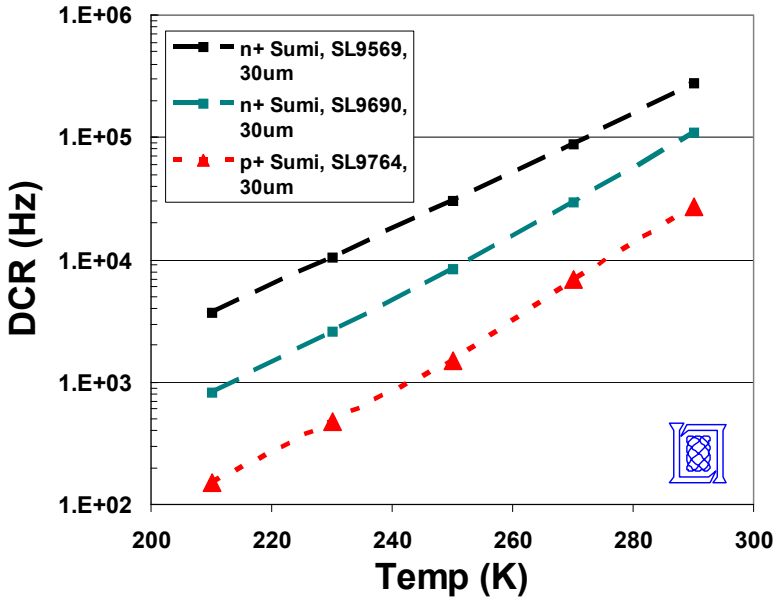

Figure 6 The temperature variation of DCR of three typical InGaAsP-InP GM APDs. As the thickness of the multiplier increases from nearly 1.0 µm to 1.6 µm, the DCR decreased dramatically, and the improvement at lower temperature is even greater than a decade. The DCR data was taken at 4V overbias on 30 µm devices at MIT-LL.

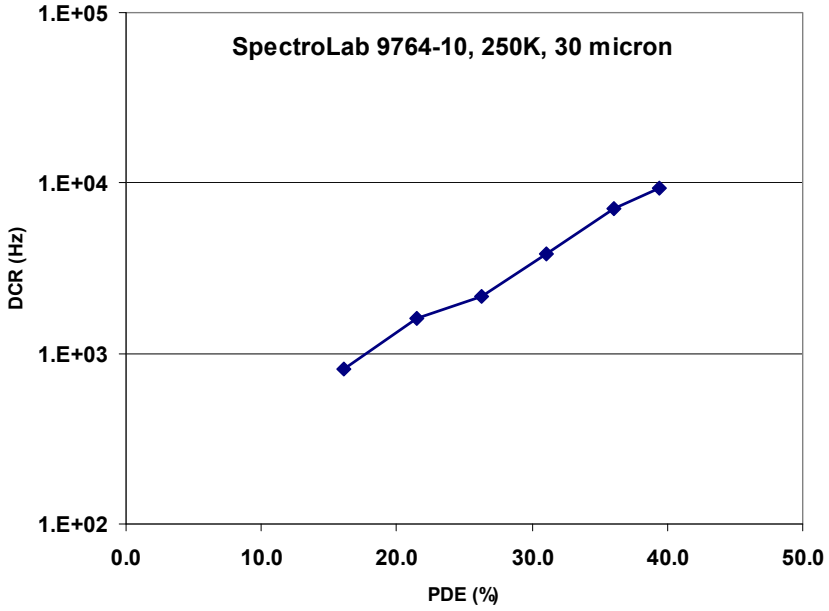

Figure 7 The DCR-vs-PDE chart of a 30-µm device of 9764 at 250 K. Nearly 40% PDE at 1.06 µm can be achieved with a DCR of 10 kHz.

6. CONCLUSIONS

In order to improve the overall performance of the InGaAsP-InP Geiger-mode APD for the 1.06 μm applications, the SAM structure was carefully analyzed and a figure of merit, DEF, was proposed. As shown in the analysis, as well as proven in experiment, a thicker InP multiplier is essential to reduce the DCR from room temperature to about 200 K. With other improvements in epitaxial growth quality and substrate, a DCR as low as 1 kHz has been demonstrated at 4V overbias at 240 ^{o}C. A nearly 40% PDE was achieved at a DCR of 10 kHz at the reduced temperature.

7. REFERENCE

1 R. J. McIntyre, "On the Avalanche Initiation Probability of Avalanche Diodes Above the Breakdown Voltage," *IEEE Transactions on Electron Devices*, vol. 20, no. 7, July, 1973.

2 S. M. Sze, *Physics of Semiconductor Devices*, New York: Wiley, 1981, pp. 520-527.

3 J.P. Donnelly, E. K. Duerr, A. McIntosh,E. A. Dauler, D.C. Oakley, S. H. Groves, C.J. Vineis, L.J. Mahoney, K.M. Molvar, P.I. Hopman, K.E. Jensen, G.M. Smith, S. Verghese, D.C. Shaver, "Design Considerations for 1.06-mm InGaAsP-InP Geiger-Mode Avalanche Photodiodes," *IEEE Journal of Quantum Electronics*, vol, 42, no. 8, August, 2006.

4 Cook, L. W.; Bulman, G. E.; Stillman, G. E., "Electron and hole impact ionization coefficients in InP determined by photomultiplication measurements," Appl. Phys. Lett., vol. 40, no. 7, pp.589-591, April, 1982.

5 C. A. Amiento and S. H. Groves, "Impact ionization in (100)-, (110)-,and (111)-oriented InP avalanche photodiodes," *Appl. Phys. Lett*., vol. 43, no. 2, pp. 333–335, July 1983.

6 S. Verghese, J.P. Donnelly, E.K. Duerr, A. McIntosh, D.C. Chapman, C.J. Vineis, G.M. Smith, J.E. Funk, K.E. Jensen, P.I. Hopman, D.C. Shaver, B.F. Aull, J.C. Aversa, J.P. Frechette, J.B. Glettler, Z.L. Liau, J.M. Mahan, L.J. Mahoney, K.M. Molvar, F.J. O'Donnell, D.C. Oakley, E.J. Ouellette, M.J. Renzi, and B. M. Tyrrell, "Arrays of InP-based Avalanche Photodiodes for Photon Counting," *IEEE J. of Selected Topics in Quantum Electronics*, vol. 13, no. 4, July/August, 2007.